



## **DC Measurement of Electrical Contacts between Strands in Superconducting Cables for the LHC Main Magnets**

D. Richter, J.D. Adam, J.M. Depond, D. Leroy and L.R. Oberli

### **Abstract**

In the LHC main magnets, using Rutherford type cable, the eddy current loss and dynamic magnetic field error depend largely on the electrical resistance between crossing ( $R_c$ ) and adjacent ( $R_a$ ) strands. Cables made of strands with pre-selected coatings have been studied at low temperature using a DC electrical method.

The significance of the inter-strand contact is explained. The properties of resistive barriers, the DC method used for the resistance measurement on the cable, and sample preparation are described. Finally the resistances are presented under various conditions, and the effect is discussed that the cable treatment has on the contact resistance.

LHC Division

ASC Pittsburgh '96

CERN  
CH - 1211 Geneva 23  
Switzerland

Geneva, 25/10/96

# DC Measurement of Electrical Contacts between Strands in Superconducting Cables for the LHC Main Magnets

D. Richter, J. D. Adam, J.-M. Depond, D. Leroy, and L. R. Oberli  
CERN, CH-1211 Geneva 23, Switzerland

**Abstract**—In the LHC main magnets, using Rutherford type cable, the eddy current loss and dynamic magnetic field error depend largely on the electrical resistance between crossing ( $R_c$ ) and adjacent ( $R_a$ ) strands.

Cables made of strands with pre-selected coatings have been studied at low temperature using a DC electrical method.

The significance of the inter-strand contact is explained. The properties of resistive barriers, the DC method used for the resistance measurement on the cable, and sample preparation are described. Finally the resistances are presented under various conditions, and the effect is discussed that the cable treatment has on the contact resistance.

## I. INTRODUCTION

The coils of the LHC dipoles and quadrupoles [1] consist of 2 layers of winding, 15 mm wide, with a different superconducting Rutherford type cable for each layer.

The inner cable of the dipoles is made of 28 strands 1.065 mm in diameter, having a Cu/SC ratio of 1.6. The outer cable is made of 36 strands 0.825 mm in diameter. The 1300 LHC twin aperture dipoles will require the fabrication of around 6600 km of superconducting cable.

The strands are annealed before coating and cabling. The cable is fabricated by passing the strands through a Turk's head, where they are strongly deformed. Sometimes diluted and volatile oil is introduced in the cable during fabrication.

A standard heat treatment (SHT) for 0.5 hour at 190 °C under pressure is used in the fabrication of the coils for gluing the polyimide insulation of the cable.

In a Rutherford type cable strands touch in 3 types of contacts: strands laying in opposite faces of the cable form crossing contacts with electrical resistances  $R_c$ , neighboring strands form (on most of the length) adjacent contacts with resistances  $R_a$ , while on the cable edges they form more complex contacts related to  $R_a$  and  $R_c$ .  $R_a$ ,  $R_c$  are defined and normalized as the resistances per one cross-over of strands. The values of these resistances are very sensitive to the fabrication process of cables and coils.

During the ramping of the LHC magnets, coupling currents are induced between the strands, resulting in dynamic distortions of the magnetic field, and in energy losses. These effects are proportional to  $dB/dt$  and inversely proportional to the contact resistance  $R_c$ . The inner layer of the LHC dipoles is the main source of field error and Joule heating.

The desired value of  $R_c$  in the main LHC magnets is limited at its minimum by constraints on the dynamic

magnetic field error and the energy losses. At its maximum, the  $R_c$  is limited by the cable stability against thermal excitations [2], and uneven current distribution between strands due to boundary-induced coupling currents [3]. Based on a theoretical study [4] and the measurement of dynamic field errors, the  $R_c$  should be maintained above 10  $\mu\Omega$ . The R&D work aims at a value of 20  $\mu\Omega$ . At the same time  $R_c$  should not be set too high for thermal stability reasons.

The effect of adjacent  $R_a$  on the magnetic field error is not significant for  $R_a > 0.2 \mu\Omega$  [5], which is valid in all applicable non-soldered cables.

The LHC strands are well defined, but the strand coating, which represents only a small part of the cable budget, has still to be optimized.

The main goal of the R&D program is: 1) to define a coating which can be industrially deposited, and well controlled either at the strand or at the cable level, and 2) to establish procedures that guarantee the desired value of  $R_c$  in functioning magnets.

## II. THE R&D PROGRAM ON CONTACT RESISTANCE AT CERN

The CERN R&D program has 3 main lines of activity:

- the testing of the physical properties of the strand with different coatings by a three contacts setup [6],
- the measurement of  $R_c$  in industrially made cables by a DC method, and simulating the various fabrication processes, which both are described in this paper,
- the determination of  $R_c$  and its distribution in the magnet coils by measurement of the loss and the dynamic magnetic field error [7].

The program incorporates the physical and chemical observation of the contact surfaces before cabling, after cabling, and after the heat treatment with and without pressure, in connection with the coil fabrication procedures. Special attention is paid to the analysis of the local deformation, and the evolution of oxides in the coatings.

The  $\text{Sn}_{95\text{wt.}}\text{Ag}_{5\text{wt.}}$  coated strands, which have been widely used in accelerator magnets and in the LHC prototypes, are being extensively studied. Other variants under evaluation are: non-coated strands, strands having a CuNi barrier, strands coated with Ni, Zn, SnNi, SnZn, SnIn, NiZn and InSb.

Special developments are pursued at the cabling level in order to fabricate and evaluate Rutherford cables with a metallic ribbon between the strand layers in the states: non-soldered, partially soldered, or soldered with a porous metal.

Similar programs exist for other machines; bare superconducting cables have been extensively studied for the RHIC [8], and for the SSC [9].

### III. PROPERTIES OF THE RESISTIVE BARRIER

The interstrand contact resistance (ICR) is controlled by the resistive barrier surrounding the strand. A layer of resistive alloy, e.g. CuNi, or a thin film of Cu oxides on the surface of the strand form a resistive barrier.

An ideal bulk material giving the  $R_c$  of  $20 \mu\Omega$  at a thickness of  $1 \mu\text{m}$  should have resistivity of  $10^{-5} \Omega\text{m}$  at 1.9 K. As an example, the barrier made of  $\text{Cu}_{70}\text{Ni}_{30}$  giving  $R_c$  of  $20 \mu\Omega$  should be as much as  $\sim 30 \mu\text{m}$  thick.

A barrier can also be made from a thin film of metal oxides. They form spontaneously or can be formed artificially on the strand surface. Some of them are semiconductors with high resistivity at low temperature. A few nm thick layer is sufficient to have the  $R_c$  of  $20 \mu\Omega$ . Most of the LHC model magnets use strands coated with  $\text{Sn}_{95\text{wt.}}\text{Ag}_{5\text{wt.}}$  which in contact with air develops a similar barrier. The metallurgical properties of  $\text{Sn}_{95\text{wt.}}\text{Ag}_{5\text{wt.}}$  are discussed in the next paragraph.

$R_c$  of cables changes during cable and magnet manufacturing, intermediate storage, and perhaps during the magnet functioning. Shaping and gluing of magnet coils (curing) changes the ICR more than any other step. Cables with bare Cu strands, ready for coil manufacturing have an  $R_c$  of  $10^2$  to  $10^3 \mu\Omega$ . After SHT curing, their  $R_c$  drops to 0.5 to  $2 \mu\Omega$ . The resistive barrier must be robust in order to keep the  $R_c$  within desired limits.

Another physical properties of the resistive barrier which should be taken into consideration are: good adhesion to the strand, low thermal Kapitza resistance to the superfluid He II, and small thickness as the barrier occupies space used otherwise by stabilizing copper. These properties are not subject of this paper.

#### A. Properties of the SnAg Coating

As an example, we resume the creation and diffusion of intermetallics and oxides in the SnAg coating, as found in literature.

The SnAg coating for the LHC is made by hot dipping the annealed strand in a  $\text{Sn}_{95\text{wt.}}\text{Ag}_{5\text{wt.}}$  bath. The coating layer is nominally 1 to  $1.5 \mu\text{m}$  thick.

Inside the strand, at the Cu/SnAg boundary, Cu diffuses into the coating and Sn diffuses into the Cu, creating CuSn intermetallics [10]: a film of the  $\text{Cu}_3\text{Sn}$  intermetallic called  $\epsilon$ -phase, and on top of it a  $\text{Cu}_6\text{Sn}_5$  intermetallic with a grain structure, called  $\eta$ -phase. At room temperature the  $\epsilon$ -phase  $\text{Cu}_3\text{Sn}$  remains limited to the Cu/coating interface, while the  $\eta$ -phase  $\text{Cu}_6\text{Sn}_5$  grows continuously through grain boundaries until the external surface of the coating is reached. If the temperature increases, the  $\epsilon$ -phase  $\text{Cu}_3\text{Sn}$  grows as a layer at the expense of the  $\eta$ -phase. Slightly

above the melting temperature of the coating ( $\sim 210^\circ\text{C}$ ) the growth of the  $\epsilon$ -phase accelerates so that it can fill the coating layer in a few minutes.

We have observed by the means of Auger depth analysis [11] that in some of the tested strands the coating was completely transformed into a  $\text{Cu}_6\text{Sn}_5$  phase, while on other tested strands some non-reacted  $\text{Sn}_{95\text{wt.}}\text{Ag}_{5\text{wt.}}$  remained at the surface.

The coating of the strand reacts with air. The type of oxide which is formed on the surface during storage or heat treatment depends on the composition of the coating. When  $\text{Sn}_{95\text{wt.}}\text{Ag}_{5\text{wt.}}$  remains on the surface, or when the  $\eta$ -phase  $\text{Cu}_6\text{Sn}_5$  intermetallic reaches the surface, oxides SnO or a mixture of SnO+SnO<sub>2</sub> are formed [12]. When  $\epsilon$ -phase  $\text{Cu}_3\text{Sn}$  exists at the surface, Cu oxide is developed.

From that description of the formation of oxide barriers in SnAg coating we can deduce that during the coating process and periods of storage, predominantly SnO barrier is formed at the surface. When the cable is fabricated through the turk's head the oxide layer is strongly modified.

In order to study the properties of the barrier formed by Cu oxides, the coating layer has first to be converted into the  $\epsilon$ -phase intermetallic by a special heat treatment.

During the magnet coil curing, the conductor is warmed up typically to  $190^\circ\text{C}$  at a pressure of  $\sim 100\text{MPa}$  for  $\sim 30$  min. The contacts between strands close hermetically under pressure. Micro-contacts flatten and oxygen easily diffuses from the contact surface inside the coating. As no additional oxygen can reach the contact, concentration of oxygen in the contact drops and so the  $R_c$  decreases, as measured in our experiments.

One of our goals was to obtain a resistive barriers being stable after coil curing.

### IV. DC ELECTRICAL METHOD FOR MEASUREMENT OF $R_c$ ON CABLE SAMPLES

We have implemented a system for DC electrical measurement of  $R_A$  and  $R_c$ . The system consist of a 4.2 K cryostat with a superconducting magnet, sample holders, DC current supplies for samples and for the superconducting magnet, and an (IBM compatible) personal computer controlling the experiment. In addition we use a hydraulic press for the sample assembly, and an electrical oven for the heat treatment of the samples.

#### A. Principle of the Measurement

The principle of the method is the measurement of the distribution of the DC voltage among the strands of a cable sample in the superconducting state, and the evaluation of  $R_A$  and  $R_c$  from this distribution. The electrical field in the sample is controlled by current injected into two opposite strands.

The electrical scheme of the sample is shown on Fig. 1. Each superconducting strand acts as an equipotential cylinder. Let us suppose that both  $R_A$  and  $R_c$  are uniform in

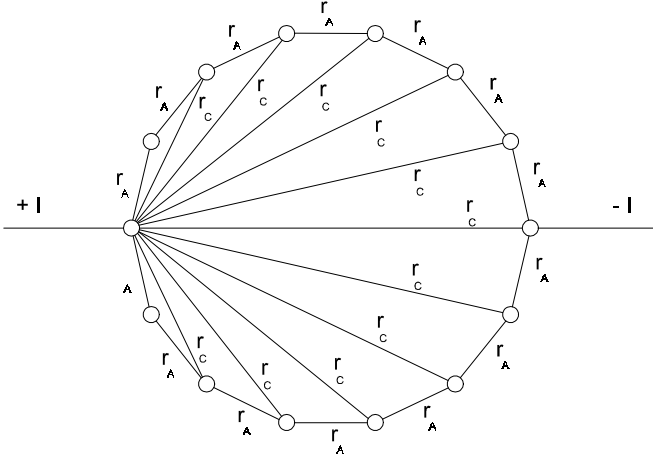


Fig. 1. Simplified electrical scheme of the cable sample. The scheme is drawn for a cable with 14 strands, which are marked with circles. The measured cables had 26, 28, and 30 strands. For the sake of clarity, the  $r_c$  resistances are shown between the strand connected to lead +I, and all other strands only. In cable these resistances exist between any two non-adjacent strands.

the sample. The complete electrical network of the cable then simplifies, and can be described using total resistances  $r_A$  and  $r_C$  between strands. The total resistance  $r_A$  between two adjacent strands is a parallel combination of  $N_s \times N_{L2}$  adjacent contacts with resistance  $R_A$ , and  $N_{L2}$  crossing contacts with resistance  $R_C$ . The total resistance  $r_C$  between two non-adjacent strands is a parallel combination of  $N_{L2}$  crossing contacts with resistance  $R_C$ .  $N_s$  is the number of strands in the cable,  $N_{L2} = 2 \times L_{\text{sample}} / L_w$ , where  $L_{\text{sample}}$  is the length of the sample, and  $L_w$  is the twist length of the cable. Electrically the sample is a polygon with strands in the nodes, adjacent resistances  $r_A$  on the sides, and crossing resistances  $r_C$  as diagonals. The current leads are connected in two opposite nodes of the polygon.

If both  $R_A$  and  $R_C$  are uniform in the sample, the voltage distribution is symmetrical. The shape of the distribution (Fig. 2.) is a function of the  $R_A/R_C$ , while the voltage  $U_I$  between strands used as current leads, is a function of both  $R_A$  and  $R_C$ . This result was independently shown in [3]. In real cable the distribution is not symmetrical as a result of the ICR changing on the cross-section of cable.

If  $R_A > 7 \times R_C$ , we consider that  $R_C$  is proportional to  $U_I$ . When that condition is not valid, we calculate a voltage distribution for trial values of  $R_A^*$  and  $R_C^*$  by solving the circuit matrix of the cable. We use  $R_A^*$  and  $R_C^*$  as parameters, and we minimize for the selected strands the square difference between the measured and calculated voltages. In that case we take into account both the varying ICR and the real geometry of the cable.

### B. Experimental Setup

The sample holder consists of a cradle, a piston, a set of pins, and an outer shrinking cylinder (Fig. 3.). The cradle and the piston are made of stainless steel, the pins are made of hardened silver steel, and the shrinking cylinder is made

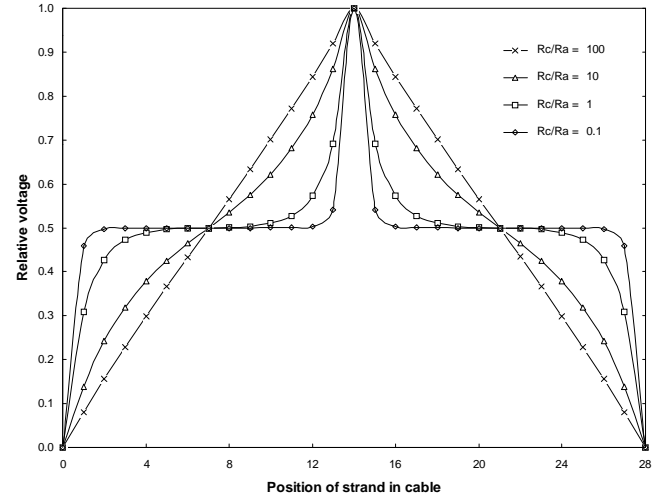


Fig. 2. Voltage distribution on a sample with homogenous  $R_A$  and  $R_C$ . The voltage is relative to the voltage  $U_I$  between the strands introducing current into the sample.

of Ti alloy. The holder has 42 mm outer diameter and is 190 mm long.

The two trapezoidal cables, insulated by a double wrap of 25  $\mu\text{m}$  thick polyimide foil, are installed into the cradle in opposite directions, so that they have an overall rectangular cross-section. The cables are compressed into the cradle via a piston with the help of a press. Pins are then installed to maintain the assembly, and the pressure is released. The shrinking cylinder is compressed perpendicularly to the longitudinal axis, and deformed to allow the insertion of the cradle with cable and piston. When the pressure on the shrinking cylinder is released, the cylinder pushes the piston against the cradle keeping the cable under pressure ( $P$ ).  $P$  is calculated from the difference in deformation of the relaxed shrinking cylinder with and without sample with the precision of 15 %. The value of  $P$  depends on the dimensions of the sample, and varies between 20 and 35 MPa. For several measurements a new sample holder was used with  $P = 50$  MPa.

Nine pairs of potential taps are attached to each sample:

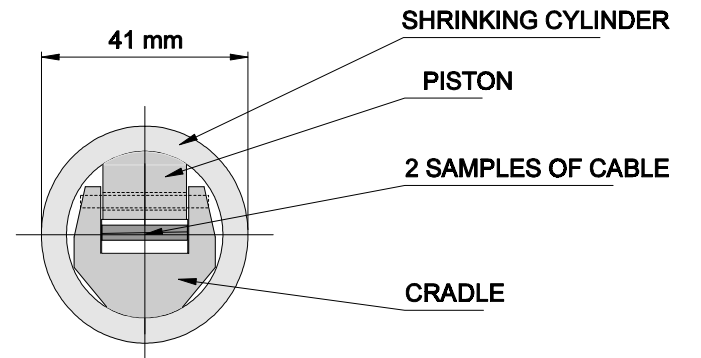


Fig. 3. The sample holder consists of the cradle, piston and the shrinking cylinder. Two samples of cable are installed in opposite directions. The holder is 190 mm long.

one pair is attached to the strands used to connect the sample to the current supply. The other pairs are used to record the potential on the 8 strands closest to the strands connected to the current supply.

The measured voltage ranges between 100 nV and 100  $\mu$ V, and is measured by a Keithley 182 nano voltmeter using a Keithley 7001 scanner. The measurement is fully controlled by a personal computer.

Magnetic field is applied parallel to the longitudinal axes of the sample by a superconducting solenoid in persistent mode.

### C. Measurement Procedure

All ICR measurements presented here were done at 4.2 K, and P of 20 to 35 MPa, unless specified otherwise.

During testing, the sample undergoes a series of different heat treatment and pressure relaxation, with the ICR measured after each step.

In order to trace the  $R_A$  and  $R_C$  evolution during magnet production, we measure the ICR of the cables: 1) as delivered, 2) after heat treatment at elevated temperature and pressure simulating the coil curing, and 3) after the pressure on the sample was relaxed overnight and restored. In order to study the properties of ICR when oxides penetrate into the strands special heat treatment is applied to the cable.

The ICR measurement starts by cooling the sample down to  $\sim 4.2$  K in a liquid Helium bath. The voltage distribution between strands of the cable is then recorded both in a magnetic field of  $B = 6$  T, and at zero magnetic field.

In order to get the voltage distribution, taps 1 to 9 are successively connected to the voltmeter via the scanner. For each tap, the voltage is recorded at current levels of: 0, 10, 0, 40, 0, 70, 0, 100, and 0 A, or 0, 2, 0, 8, 0, 14, 0, 20, and 0 A, in both polarities. The voltage measured at 0 A, and the standard deviation of each measurement are used to monitor the drift and noise.

The measured  $R_C$  is an average value of  $R_C$  of about 1200 contacts. The error of the measured average  $R_C$  is 0.005  $\mu\Omega$  or 0.03 %, whatever is bigger. This error is not related to the spread of the ICR in the cable. However the spread of the average  $R_C$  measured on several samples of the same cable is related to the spread of individual  $R_C$ , and could be used to estimate it.

## V. RESULTS OF $R_C$ MEASUREMENT PERFORMED ON CABLE SAMPLES

The comparison between the  $R_C$  measurements on cable samples and the measurements in magnets is given in paper [7]. The correlation between the measurements on cable samples and the measurements on strands is discussed in paper [6].

With the exception of cables with resistive core and soldered cables, the measurements of ICR have shown that  $R_A \gg R_C$ . We therefore limit our presentation to  $R_C$  for all the other measured cables.

## VI. CABLES WITH STRANDS WITHOUT COATING

### A. Effect of Heat Treatment under Pressure

The fit of the measured data for 25, 165, 190, 215, 246 C. shows exponential decrease of resistance with the temperature of the heat treatment (Fig. 4.):

$R_C = 152 \times \exp(-0.0297 \times \theta)$  [ $\mu\Omega$ ] for cable No. 2184, and  $R_C = 1590 \times \exp(-0.0363 \times \theta)$  [ $\mu\Omega$ ] for cable No. 525. In both cases, data are for heat treatment of 1 hour at temperature  $\theta$  and  $P = 28$  MPa, and  $B = 0$  T. For example the cable No. 2184 has  $R_C = 0.54 \mu\Omega$ , while cable No. 525 has  $R_C = 1.6 \mu\Omega$  after SHT. These results indicate that  $R_C$  is influenced by the cable manufacturing, since the cables were made by different suppliers from the same strands.

The residual  $R_C$  after heat treatment for 3 hours at 250 C, and  $P = 23$  to 30 MPa was 0.078  $\mu\Omega$  (No. 2184, 0T) and 0.16  $\mu\Omega$  (No. 525, 0T). These results indicate that if contacts stay well closed during the heat treatment, natural Cu oxides diffuse into the copper so that the electrical resistance of the barrier decreases. To obtain an  $R_C$  value needed for the LHC magnets, the oxide layer has to be produced by relaxing the cable pressure during the coil curing as has been implemented in the RHIC machine magnet construction [8].

### B. Comparison with Measurement in Magnets

The mean value of  $R_C$  measured in 3 model dipoles made with the cable coming from the same supplier (No. 2184) is above 30  $\mu\Omega$  [7]. This high value of  $R_C$  in the magnets indicates that new oxide layers must have been produced between the contacts during curing.

The rate of creation for oxide layers on Cu is as high as 5 nm/min at 170 C [8]. The problem which has still to be solved is the exact procedure (temperature and pressure cycle) for controlling the equal distribution of the oxide inside the contacts and all over the length of cables during the coil curing. Another source of non-uniform distribution concerning the Cu oxide layers could be its fragility as shown in [6]. Moreover the Kapitza thermal resistance is

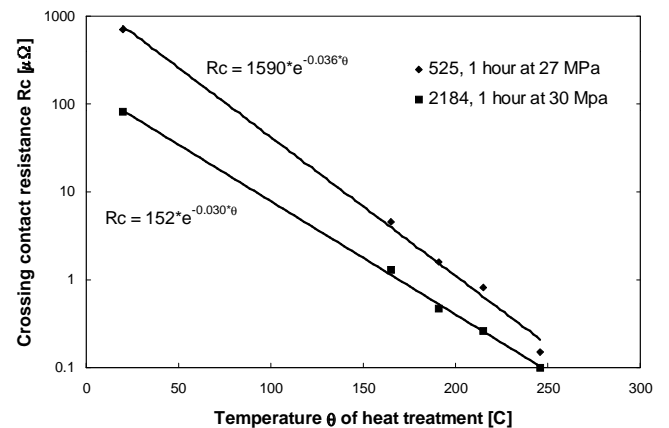


Fig. 4. Crossing contact resistance  $R_C$  of cables No. 525 and No. 2184 with non-coated strands.

very sensitive to the state of the Cu surface that could be harmful to the stability of LHC magnets operating at 1.9 K.

#### C. Evolution of $R_c$ with Time at Room Temperature

Two cable samples (No. 2184) which have been treated respectively at 190 and 250 C and kept under a pressure of 28 MPa, showed an  $R_c$  decrease of 17 and 10 % after 42 days. The results of these measurement indicate that the oxide is still diffusing into Cu at room temperature and continues to influence  $R_c$ .

#### D. Influence of the Magnetic Field

The variation with the magnetic field of  $R_c$  between 0 and 6 T is the same for both cables and seems to depend mainly on the internal strand geometry and copper quality. The measured variation  $\frac{R_c(6T) - R_c(0T)}{R_c(0T)}$  was 0.11, 0.31, 0.44 for the different heat treatment of 160, 190, and 215 C. The Kohler's rule for copper having a residual resistivity ratio  $rrr = 140$  and 33 would give a resistance variation of 2 and 0.5 between 0 and 6 T.

### VII. CABLES WITH STRANDS WITH CuNi RESISTIVE BARRIERS

Cable No. 2188 with strands having a CuNi resistive barrier was compared with cable No. 2192 having similar strands without barrier. The CuNi barrier was  $\sim 13 \mu\text{m}$  thick and was embedded in the outer Cu shell of the strand  $\sim 50 \mu\text{m}$  deep from the strand surface. Strands of both cables were coated with  $\sim 1 \mu\text{m}$  of  $\text{Sn}_{95\text{wt}}\text{Ag}_{5\text{wt}}$ . The cables as received had  $R_c = 11 \mu\Omega$  (No. 2188, 13MPa, 0T) and  $R_c = 13 \mu\Omega$  (No. 2192, 13MPa, 0T). Heat treatment of 250 C at 13MPa for 2 hours was applied to both cables in order to distinguish the net contribution of the CuNi barrier.  $R_c$  dropped to  $R_c = 2.4 \mu\Omega$  (No. 2188, 13MPa, 0T) and  $R_c = 0.8 \mu\Omega$  (No. 2192, 13MPa, 0T) respectively.

The difference of  $1.6 \mu\Omega$  is due to the CuNi barrier. Calculation based on the bulk resistivity of  $\text{Cu}_{70}\text{Ni}_{30}$  and contact dimensions suggests that  $R_c$  would be  $17 \mu\Omega$  if a  $\text{Cu}_{70}\text{Ni}_{30}$  barrier of  $25 \mu\text{m}$  would be put at the surface of the strand.

### VIII. CABLES WITH STRANDS COATED WITH $\text{Sn}_{95\text{wt}}\text{Ag}_{5\text{wt}}$

The  $R_c$  values of the cables, as received, vary from 1.7 to  $3.7 \mu\Omega$  (cables No. 2193, 01B0222, 01E0104S), and from 11 to  $30 \mu\Omega$  (cables No. 2191, 2192, 01B234A2, 01B234C2, 01D6001), for a pressure between 20 and 50 MPa.

Releasing and re-applying the pressure on the cable at room temperature and reinstalling the sample in the holder does not change  $R_c$ .

#### A. Effect of Heat Treatment under Pressure

Heat treatment under pressure diminishes  $R_c$  following the exponential law  $R_c = \alpha \times \exp(-\beta \times \theta)$  [ $\mu\Omega$ ], with  $\theta$  the temperature of the heat treatment at full pressure. The

coefficient  $\beta$  is rather constant for all samples ( $\beta = 0.010 \pm 0.001 \text{ K}$ ), while the coefficient  $\alpha$  depends on the sample as shown in the Fig. 5:

- $\alpha = 23.0 \mu\Omega$  for cable No. 2191, 2 hours at 11 MPa,
- $\alpha = 16.8 \mu\Omega$  for cable No. 2192, 2 hours at 11 MPa,
- $\alpha = 5.00 \mu\Omega$  for cable No. 2192, 2 hours at 25 MPa,
- $\alpha = 3.27 \mu\Omega$  for cable No. 2193, 1 hour at 27 MPa.

After the SHT the  $R_c$  value is a factor 7 smaller than before the SHT.

In order to understand in general the evolution of  $R_c$  due to the heat treatment and pressure cycles we compared measurements on samples No. 01B0222, 01D6001, and 01E0104S produced by different manufacturers.  $R_c$  of cables as received ranged between 1 and  $25 \mu\Omega$ , and  $R_c$  during the testing ranged between 0.6 and  $125 \mu\Omega$ . We found that for all 3 cables (at  $P = 19$  to 27 MPa):

- heat treatment for 1.5 hour at 110 C decreases  $R_c$  to  $R_{c0} / 1.9$ ,
- heat treatment for 1.5 hour at 110 C and for 1.5 hour at 140 C decreases  $R_c$  to  $R_{c0} / 3.1$ ,
- heat treatment for 0.5 hour at 190 C decreases  $R_c$  to  $R_{c0} / 7.0$ .

$R_{c0}$  is the resistance before heat treatment.

If the pressure is released after a 0.5 hour heat treatment at 190 C,  $R_c$  increases to  $R_{c0} + 14 \mu\Omega$ . The standard deviation of all these relations was 30%. One exception was observed in sample No. 01E0104S; after pressure release  $R_c$  reached its value before SHT but did not increment by  $14 \mu\Omega$ . If one subsequent SHT under pressure on the same sample is made,  $R_c$  will decrease by the already mentioned factor of 7.

#### B. Effect of Stimulated Oxidation at Room Temperature

In order to understand how different test operations modify  $R_c$ , we performed a series of measurements on samples from cable No. 01E0104S. We found that humidity

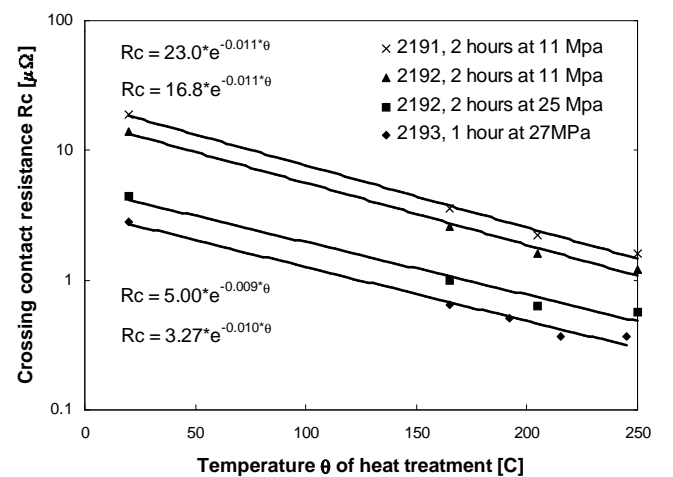


Fig. 5 Crossing contact resistance  $R_c$  of cables No. 2191, 2192, and 2193 with  $\text{Sn}_{95\text{wt}}\text{Ag}_{5\text{wt}}$  coated strands.

condensing on the sample after it has been removed from the cryostat increases the resistive barrier.

Experiments show that  $R_c$  of barriers formed by humidity at room temperature decreases more after the first SHT, than  $R_c$  of barriers formed at 190 C.

### C. Effect of Heat Treatment without Pressure and Stimulated Oxidation

Heat treatment at 190 C without any pressure has been performed on cables No. 01B0222, 01D6001, and 01E0104S and lead to an increase by 14  $\mu\Omega$  independently of the strand and cable manufacturing, and even of the previous history of the cable. If one subsequent heat treatment with pressure on the same sample is made, the  $R_c$  will decrease by the already mentioned factor of 7. These measurements show that relaxing the pressure after SHT, or heat treating without pressure has the same effect on  $R_c$ .

We performed a series of experiments on samples from cables No. 01B234A2, 01B234C2, and 01E0104S in order to understand what treatment causes the increase of the resistive barrier. We found for cable No. 01E0104S that during heat treatment in dry air at 190 C, a protecting layer of oxides is formed on the strand surface. This layer prevents further oxidation, and thereby does not allow to increase  $R_c$  by more than 14  $\mu\Omega$  even after 2 hours heat treatment. If one subsequent heat treatment with pressure on the same sample is made,  $R_c$  will decrease by the factor of 7.

When the sample (measured on cable No. 01B234A2, 01B234C2, and 01E0104S) was treated at 190 C in air containing water vapor, the  $R_c$  barrier continued to grow. The increment in  $R_c$  after 4 hours of heat treatment was 58 and 66  $\mu\Omega$  (sample No. 01B234A2), and 71 and 81  $\mu\Omega$  (sample No. 01B234C2).

After a first SHT, following the heat treatment in the air containing water vapor, the 2 samples No. 01B234A2 reached  $R_c=17$  and 13  $\mu\Omega$ , while the samples No. 01B234C2 reached  $R_c=22$  and 23  $\mu\Omega$ . After the 2<sup>nd</sup> SHT heat treatment, which immediately followed the first one,  $R_c$  decreased only by 2 to 4%. These results indicate that the oxide formed by using water vapor penetrates deeper in the coating and the concentration gradient flattens. The rate of the oxide diffusion into the coating slows then down, and  $R_c$  becomes constant in the range of 17 to 23  $\mu\Omega$ , independently of the following heat treatment.

### IX. CABLES WITH STRANDS COATED WITH Ni

Strands of the cable No. 531 have a Ni electroplated layer of 1  $\mu\text{m}$  thickness. The  $R_c$  of the cable as received was 318 and 386  $\mu\Omega$ , at  $B = 0$  and  $P = 30$  and 25 MPa respectively.

In the first series of heat treatment the sample shows a linear decrease of  $R_c$ :  $R_c = -0.850 \times \theta + 216$  [ $\mu\Omega$ ], with temperature. Conditions of the measurements are: heat treatment of 1 hour at temperature  $\theta$  and  $P = 30$  MPa,  $B = 0$  T. The fit is based on data for 20, 165, 190, 213, and

246 C. The linear relation results in a decrease in ICR smaller than for the previously described coatings.

After releasing the pressure, an increase of  $R_c$  occurs and the value can be close to or even well above the  $R_c$  value of the as received cable. A subsequent heat treatment shows a reduced linear decrease:  $R_c = -0.583 \times \theta + 197$  [ $\mu\Omega$ ]. Conditions of the measurements are: heat treatment of 1 hour at temperature  $\theta$  and  $P = 28$  MPa,  $B = 0$  T. The fit is based on data for 165, 190, 215, and 246 C.

The effect of the second heat treatment can be expressed by a ratio between the initial and final values of  $R_c$ . The ratio is a constant for a given heat treatment and cable, and does not depend on the initial value. For the heat treatment of 1 hour at 245 C and 24 MPa the ratio was 3.8 to 4.5 while the initial  $R_c$  varied between 185 and 1140  $\mu\Omega$ .

Samples treated at 190 and 250 C were re-measured after 42 days at  $P = 26$  MPa. They showed a small increase of  $R_c$  with time.

### X. CABLES WITH STRANDS COATED WITH $\text{Sn}_{95\text{wt.}}\text{Ag}_{5\text{wt.}}$ AND WITH A METALLIC CORE IN THE CABLE

Cable No. 533 is made of  $\text{Sn}_{95\text{wt.}}\text{Ag}_{5\text{wt.}}$  coated strands and has a 25  $\mu\text{m}$  thick stainless steel core [13]. After a heat treatment of 1 hour at 165 C and 31 MPa, the contact resistance of the two samples was equal to  $R_c = 109$  and 122  $\mu\Omega$ , and  $R_A = 4.8$  and 5.1  $\mu\Omega$  respectively. The high  $R_c$  value obtained with the stainless steel core is probably due to an oxide barrier formed on the core.

Cable No. 534 has a 25  $\mu\text{m}$  thick Ti core and  $\text{Sn}_{95\text{wt.}}\text{Ag}_{5\text{wt.}}$  coated strands. After heat treatment of 1 hour at 165 C and 31 MPa, the contact resistance of the two samples was equal to  $R_c = 50$  and 54  $\mu\Omega$ , and  $R_A = 2.6$  and 3.1  $\mu\Omega$  respectively.

Partial soldering of the cored cables with  $\text{Sn}_{95\text{wt.}}\text{Ag}_{5\text{wt.}}$  has reduced the  $R_A$  to 0.14  $\mu\Omega$ .

### XI. CABLE FILLED WITH POROUS METAL

Two samples of cable with non-coated strands filled and soldered with a mixture of Ag powder and  $\text{Sn}_{95\text{wt.}}\text{Ag}_{5\text{wt.}}$  solder [13] were measured.

As received the cable had  $R_c=3.7$   $\mu\Omega$  for both samples, and  $R_A=49$  and 67  $\mu\Omega$ . In a sequence of heat treatments of 1.5 hour/110 C/27 MPa, 1.5 hour/140 C/27 MPa, pressure relaxation and application, and 0.5 hour/190 C/29 MPa,  $R_c$  of the first sample grew steadily from 3.8 to 4.3  $\mu\Omega$ , while  $R_A$  first dropped to 3.8  $\mu\Omega$  and then grew steadily to 6.5  $\mu\Omega$ .  $R_c$  of the second sample first dropped to 1.5  $\mu\Omega$  and then remained stable, while  $R_A$  first dropped to 2.3  $\mu\Omega$  and then grew to 2.8  $\mu\Omega$ . The presence of the core in the cable would increase the crossing contact resistance  $R_c$  by about 100  $\mu\Omega$ .

### XII. CONCLUSIONS

Table I. shows the typical values for the  $R_c$  obtained with the cables as received and after the heat treatment for 0.5 hour at 190 C under 20 to 30 MPa. Also shown are

results for the heat treatment for 0.5 hour at 190 C without pressure, and results after special heat treatment.

The resistive barrier in bare Cu strands readily drops after heat treatment to very low values. We did not try to produce the high  $R_c$  barrier that would result in  $R_c=20 \mu\Omega$  after SHT, because the inconvenience of such a barrier in the magnet manufacturing is the strong  $R_c$  increase if pressure is released after the magnet coil has been cured.

An external CuNi barrier could provide the desired  $R_c$  increment independent on coil curing. The inconvenience is the occupation by CuNi of part of the space otherwise used by Cu, with possible consequences for thermal stability and magnet protection.

The  $R_c$  of  $\text{Sn}_{95\text{wt.}}\text{Ag}_{5\text{wt.}}$  coated strands can be increased by chemical oxidation at elevated temperature to about 100 to 200  $\mu\Omega$ . Coils made from such a cable will have the desired  $R_c$  after curing. The  $R_c$  will not change after longer or repeated curing cycles. Even if the pressure is locally released,  $R_c$  will remain below 120 to 220  $\mu\Omega$ . Moreover, a heat treatment step could be foreseen in the cable manufacturing, that would decrease the cable  $R_c$  to the stable value, and make it insensitive to (even repeated) normal curing procedures.

In conclusion on  $\text{Sn}_{95\text{wt.}}\text{Ag}_{5\text{wt.}}$  coating,  $R_c = 20 \mu\Omega$  have been obtained by intervening either in the curing cycle or in the cable fabrication.

Strands coated with Ni show  $R_c = 50 \mu\Omega$ . More information is still necessary to know the effect of the oxides as well as about the spread of results for coatings prepared by different manufacturers. A model dipole magnet with a Ni plated cable will be fabricated at CERN.

The evaluation of cored cables is going on, from the fabrication possibilities, and the magnet stability point of views.

Other potentially useful coatings have been tested using the three point method [6].

#### ACKNOWLEDGMENT

The authors thank to Drs. L. Evans, J. P. Gourber, R. Perin for their constant interest. They are very grateful to A. Ghosh who initiated the VI measurements, to A. P. Verweij, M. N. Wilson, R. Wolf for their advises and all the fruitful discussions. They would like to thank in particular Z. Charifouline (IHEP), C-H. Denarié, Y. Liu, J-L. Servais, J. Stott, for their daily efficient support.

Special thanks to A. McInturff and R. Scanlan (LBNL) who are fabricating the special cables.

Thanks as well to the companies fabricating the superconducting cables for the LHC: GEC ALSTHOM (F), OUTOKUMPU (SF), Europa Metalli (I), Vacuum-schmelze (D).

#### REFERENCES

[1] *The Large Hadron Collider - Conceptual Design*, CERN/AC/95-05, 1995.

**TABLE I.**  
COMPARISON OF TYPICAL  $R_c$  VALUES FOR DIFFERENT COATINGS  
AND SURFACE CONDITION,  $P = 25 \text{ MPa}$

Type of strand	Condition of the cable				
	Cable as received	After heat treatment: 190 C, 0.5 hour full pressure	After oxidation heat treatment: 190 C, 0.5 hour without pressure	Accelerated oxidation	
				Cable as received	After heat treatment: 190 C, 0.5 hour full pressure
	Crossing contact resistance Rc [μΩ]				
Bare strands	80 - 700	0.5 - 1.6	-	-	-
Strands coated with SnAg	1.7 - 30	0.5 - 4.5	15 - 20	> 70	17 - 23
Internal CuNi barrier 13 μm thick	1.6 μΩ + Rc of the coating				
External CuNi barrier, 30 μm thick, calculated	20 μΩ + Rc of the coating				
Strands coated with Ni	320	55	> 300	-	-
Strands coated with SnAg, stainless steel core in cable	-	115	-	-	-

- [2] M. N. Wilson, R. Wolf, "Calculation of minimum quench energies in Rutherford cables", presented at this conference.
- [3] A. P. Verweij, *Electrodynamics of Superconducting Cables in Accelerator Magnets*. PhD thesis, Universiteit Twente Enschede, 1995.
- [4] A. P. Verweij, R. Wolf, "Field errors due to inter-strand coupling currents in the LHC dipole and quadrupole", CERN Internal Note AT/MA 94-97, 1995.
- [5] A. P. Verweij, CERN, personal communication.
- [6] J-M. Depond, D. Leroy, L. Oberli, D. Richter, "Examination of contacts between strands by electrical measurement and topographical analysis", presented at this conference.
- [7] R. Wolf, D. Leroy, D. Richter, A. P. Verweij, L. Walckiers, "Determination of interstrand contact resistance from loss and field measurements in LHC dipole prototypes and correlation with measurements on cable samples", presented at this conference.
- [8] A. K. Ghosh, "Interstrand resistance studies of oxidized superconducting wires", AD/SSC/Tech. No. 103, BNL, 1992.
- [9] V. T. Kovachev, M. J. Neal, D. W. Capone II, W. J. Carr, Jr, C. Swenson, "Interstrand resistance of SSC magnets", Cryogenics, Vol. 34, pp. 813-820, No. 10, 1994.
- [10] F. Bartels, J. W. Morris, Jr., G. Dalke, W. Gust, "Intermetallic phase formation in thin solid-liquid diffusion couples, Journal of Electronic Materials, Vol 23, pp. 787-790, No. 8, 1994.
- [11] J. D. Adam, J. P. Bacher, R. Cosso, J. M. Dalin, D. Lacarrère, and G. Sgobba, "Caracterisation du revetement d'étain sur la gaine en cuivre des cables supraconducteurs pour applications au LHC", CERN, Rapport intermédiaire MT-SM-MI/95-015/SS, 1995.
- [12] H. L. Reynolds, J. W. Morris, Jr., "The role of intermetallics in wettability degradation", Journal of Electronic Materials, Vol. 24, pp. 1429-1434, No. 10, 1995.
- [13] J. D. Adam, D. Leroy, L-R. Oberli, D. Richter, M. N. Wilson, R. Wolf, H. Higley, A. D. McInturff, R. M. Scanlan, A. Nijhuis, H. H. J. Ten Kate, and S. Wessel, "Rutherford cables with anisotropic transverse resistance", presented at this conference.